

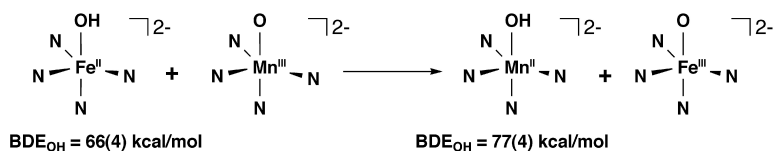
Article

## Monomeric Mn and Fe Complexes with Terminal Hydroxo and Oxo Ligands: Probing Reactivity via O–H Bond Dissociation Energies

Rajeev Gupta, and A. S. Borovik

*J. Am. Chem. Soc.*, **2003**, 125 (43), 13234-13242 • DOI: 10.1021/ja030149I • Publication Date (Web): 04 October 2003

Downloaded from <http://pubs.acs.org> on March 30, 2009



### More About This Article

Additional resources and features associated with this article are available within the HTML version:

- Supporting Information
- Links to the 11 articles that cite this article, as of the time of this article download
- Access to high resolution figures
- Links to articles and content related to this article
- Copyright permission to reproduce figures and/or text from this article

[View the Full Text HTML](#)



**ACS Publications**  
 High quality. High impact.

## Monomeric Mn<sup>III/II</sup> and Fe<sup>III/II</sup> Complexes with Terminal Hydroxo and Oxo Ligands: Probing Reactivity via O–H Bond Dissociation Energies

Rajeev Gupta and A. S. Borovik\*

Contribution from the Department of Chemistry, University of Kansas, Lawrence, Kansas 66045

Received March 4, 2003; E-mail: aborovik@ku.edu

**Abstract:** Non-heme manganese and iron complexes with terminal hydroxo or oxo ligands are proposed to mediate the transfer of hydrogen atoms in metalloproteins. To investigate this process in synthetic systems, the monomeric complexes  $[M^{III}H_3(OH)]^{-2-}$  and  $[M^{III}H_3(O)]^{2-}$  have been prepared, where  $M^{III/II} = Mn$  and  $Fe$  and  $[H_3]^{3-}$  is the tripodal ligand, tris(*N*-*tert*-butylureaylato)-*N*-ethyl)aminato. These complexes have similar primary and secondary coordination spheres, which are enforced by  $[H_3]^{3-}$ . The homolytic bond dissociation energies ( $BDE_{O-H}$ ) for the  $M^{III/II}-OH$  complexes were determined, using experimentally obtained values for the  $pK_a(M-OH)$  and  $E_{1/2}$  measured in DMSO. This thermodynamic analysis gave  $BDE_{O-H}$  of 77(4) kcal/mol for  $[Mn^{III}H_3(O-H)]^{2-}$  and 66(4) kcal/mol for  $[Fe^{III}H_3(O-H)]^{2-}$ . For the  $M^{III/II}-OH$  complexes,  $[Mn^{III}H_3(OH)]^-$  and  $[Fe^{III}H_3(OH)]^-$ ,  $BDE_{O-H}$  of 110(4) and 115(4) kcal/mol were obtained. These  $BDE_{O-H}$  were verified with reactivity studies with substrates having known  $X-H$  bond energies ( $X = C, N, O$ ). For instance,  $[Fe^{III}H_3(OH)]^{2-}$  reacts with a TEMPO radical to afford  $[Fe^{III}H_3(O)]^{2-}$  and TEMPO-H in isolated yields of 60 and 75%, respectively. Consistent with the  $BDE_{O-H}$  values for  $[Mn^{III}H_3(OH)]^{2-}$ , TEMPO does not react with this complex, yet TEMPO-H ( $BDE_{O-H} = 70$  kcal/mol) reacts with  $[Mn^{III}H_3(O)]^{2-}$ , forming TEMPO and  $[Mn^{III}H_3(OH)]^{2-}$ .  $[Mn^{III}H_3(O)]^{2-}$  and  $[Fe^{III}H_3(O)]^{2-}$  react with other organic substrates containing C–H bonds less than 80 kcal/mol, including 9,10-dihydroanthracene and 1,4-cyclohexadiene to produce  $[M^{III}H_3(OH)]^{2-}$  and the appropriate dehydrogenated product in yields of greater than 80%. Treating  $[Mn^{III}H_3(O)]^{2-}$  and  $[Fe^{III}H_3(O)]^{2-}$  with phenolic compounds does not yield the product expected from hydrogen atom transfer but rather the protonated complexes,  $[Mn^{III}H_3(OH)]^-$  and  $[Fe^{III}H_3(OH)]^-$ , which is ascribed to the highly basic nature of the terminal oxo group.

### Introduction

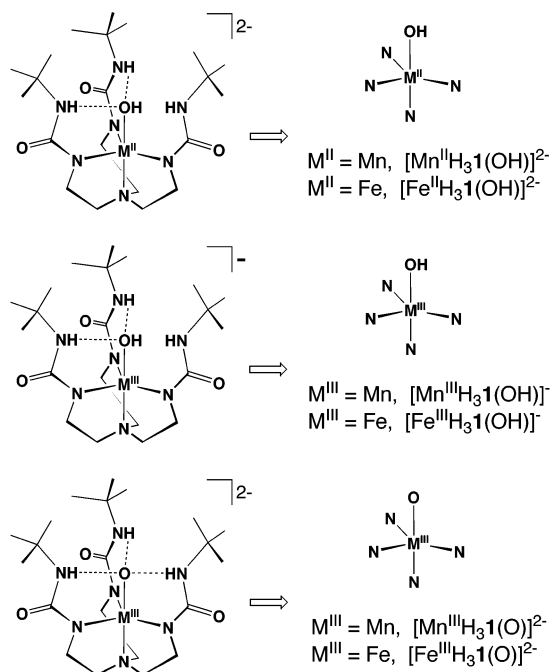
Metal ion mediated transfer of a hydrogen atom (H-atom) is a fundamental process in biology. In many cases, an  $M-O(H)$  unit, residing in the active site of a metalloprotein, has been directly implicated in H-atom transfer. For instance, the non-heme iron enzyme lipoxygenase is proposed to initiate the oxidation of unsaturated fatty acids by transfer of an H-atom from substrate to an active site  $Fe(III)-OH$  center, leading to the formation of 1-hydroperoxy-*trans,cis*-2,4-dienes.<sup>1</sup> An analogous pathway has been suggested to be operative in the recently isolated manganese-containing lipoxygenase.<sup>2</sup> The hydroxylase component of methane monooxygenase proceeds through a high valent dinuclear iron-oxo core (compound Q), which is proposed to abstract an H-atom from methane, leading to methanol production.<sup>3</sup> A related core structure is found in the R2 unit of ribonucleotide reductase (compound X) and is involved in the transfer of an H-atom from tyrosine Y122 to initialize the radical transfer pathway ultimately responsible for the reduction of sugar

units in ribonucleotides.<sup>4</sup> The reverse reaction has been suggested for the conversion of water to dioxygen in the oxygen-evolving complex (OEC) of photosystem II, where an H-atom from a  $Mn-OH$  moiety is transferred to a tyrosine radical,  $Yz^{\cdot}$ .<sup>5</sup>

One method to probe this type of H-atom transfer makes use of the homolytic bond dissociation energies of  $MO-H$  bonds ( $BDE_{O-H}$ ) in the condensed phase. Mayer has pioneered this approach in synthetic systems and shown that  $BDE_{O-H}$  are reliable predictors for the reaction of  $M-O(H)$  species with substrates containing  $X-H$  bonds.<sup>6,7</sup>  $BDE_{O-H}$  for complexes related to metalloproteins have now been reported, such as

- (1) Nelson, M. J.; Seitz, S. P. In *Active Oxygen in Biochemistry*; Valentine, J. S., Foote, C. S., Greenberg, A., Liebman, J. F., Eds.; Blackie Academic & Professional: London, 1995; Vol. 3.
- (2) Su, C.; Sahlin, M.; Oliw, E. H. *J. Biol. Chem.* **2000**, *275*, 18830–18835.
- (3) (a) Merckx, M.; Kopp, D. A.; Sazinsky, M. H.; Blazyk, J. L.; Müller, J.; Lippard, S. J. *Angew. Chem., Int. Ed.* **2001**, *40*, 2782–2807. (b) Que, L., Jr.; Tolman, W. B. *Angew. Chem., Int. Ed.* **2002**, *41*, 1114–1137.

- (4) (a) Wallar, B. J.; Lipscomb, J. D. *Chem. Rev.* **1996**, *96*, 2625–2657 and references therein. (b) Feig, A. L.; Lippard, S. J. *Chem. Rev.* **1994**, *94*, 759–805 and references therein. (c) Stubbe, J. *J. Biol. Chem.* **1990**, *265*, 5329.
- (5) (a) Tommos, C.; Babcock, G. T. *Acc. Chem. Res.* **1998**, *31*, 18–25 and references therein. (b) Gilchrist, M. L., Jr.; Ball, J. A.; Randall, D. W.; Britt, R. D. *Proc. Natl. Acad. Sci. U.S.A.* **1995**, *92*, 9545–9549. (c) Tang, X.-S.; Ball, J. A.; Randall, D. W.; Force, D. A.; Diner, B. A.; Britt, R. D. *J. Am. Chem. Soc.* **1996**, *118*, 7638–7639. (d) Pecoraro, V. L.; Baldwin, M. J.; Caudle, M. T.; Hsieh, W.-Y.; Law, N. A. *Pure Appl. Chem.* **1998**, *70*, 925–929.
- (6) (a) Gardner, K. A.; Mayer, J. M. *Science* **1995**, *269*, 1849–1851. (b) Gardner, K. A.; Kuehnert, L. L.; Mayer, J. M. *Inorg. Chem.* **1997**, *36*, 2069–2078. (c) Wang, K.; Mayer, J. M. *J. Am. Chem. Soc.* **1997**, *119*, 1470–1471. (d) Mayer, J. M. *Acc. Chem. Res.* **1998**, *31*, 441–450 and references therein. (e) Mayer, J. M. In *Biomimetic Oxidations Catalyzed by Transition Metal Complexes*; Meunier, B., Ed.; Imperial College Press: London, 2000; pp 1–43 and references therein.

**Chart 1.** Structures and Nomenclature of the M<sup>III</sup>–OH and M<sup>III</sup>–O Complexes

manganese complexes with bridging hydroxo (e.g.,  $\text{Mn}(\mu\text{-OH})_2\text{Mn}$ )<sup>8</sup> or terminal water groups<sup>9</sup> and iron species with methanol ligands.<sup>10</sup>

Our group has been evaluating the  $\text{BDE}_{\text{S}_{\text{O}-\text{H}}}$  of monomeric complexes containing M<sup>III</sup>–OH units ( $M^{\text{III/II}} = \text{Mn}$  and  $\text{Fe}$ ).<sup>11</sup> These types of complexes are often difficult to prepare because the hydroxo ligands have a strong propensity to bridge between manganese and iron centers. To circumvent bridging by hydroxide ions, we have developed the tripodal ligand tris(*N*-*tert*-butylureayl)-*N*-ethyl]amine ([H<sub>6</sub>I]), which utilizes three *N*-ethylene-*N*'-*tert*-butyl urea groups that radiate from a nitrogen atom.<sup>12</sup> Binding to a late 3d transition metal ion occurs after deprotonation of the NH-ethylene nitrogen atoms to yield species that readily form complexes with terminal oxo or hydroxo ligands (Chart 1). One advantage of this ligand system is its control of the secondary coordination sphere by forming a constrained hydrogen bond cavity around the M–O(H) units. Here, we present our findings for the  $\text{BDE}_{\text{S}_{\text{O}-\text{H}}}$  of this series of  $[\text{M}^{\text{III}}\text{H}_3\text{1}(\text{OH})]^{-}$  and  $[\text{M}^{\text{III}}\text{H}_3\text{1}(\text{O})]^{2-}$  complexes, where  $M^{\text{III/II}} = \text{Fe}$  and  $\text{Mn}$ . Furthermore, the reactivity of these complexes, along with the related M<sup>III</sup>–oxo complexes,  $[\text{Mn}^{\text{III}}\text{H}_3\text{1}(\text{O})]^{2-}$

and  $[\text{Fe}^{\text{III}}\text{H}_3\text{1}(\text{O})]^{2-}$ , are described. We show that  $[\text{Mn}^{\text{II}}\text{H}_3\text{1}(\text{O}-\text{H})]^{2-}$  has a stronger O–H bond compared to the analogous  $[\text{Fe}^{\text{II}}\text{H}_3\text{1}(\text{O}-\text{H})]^{2-}$ , which is corroborated by reactivity studies. Moreover, the M<sup>III</sup>–OH complexes,  $[\text{Mn}^{\text{III}}\text{H}_3\text{1}(\text{OH})]^{-}$  and  $[\text{Fe}^{\text{III}}\text{H}_3\text{1}(\text{OH})]^{-}$ , have similar  $\text{BDE}_{\text{S}_{\text{O}-\text{H}}}$  that are significantly greater than those reported for other metal bonded hydroxides.

## Experimental Section

**Preparative Methods and Syntheses.** All reagents were purchased from commercial sources and used as received, unless otherwise noted. Anhydrous solvents were purchased from Aldrich. Dioxxygen was dried on a Drierite gas purifier that was purchased from Fisher Scientific. The preparations of all metal complexes were conducted in a Vacuum Atmosphere drybox under an argon atmosphere. The syntheses of H<sub>6</sub>I, K<sub>2</sub>[M<sup>III</sup>H<sub>3</sub>1(O)], K<sub>2</sub>[M<sup>III</sup>H<sub>3</sub>1(OH)], K[M<sup>III</sup>H<sub>3</sub>1(OH)], and TEMPO–H followed literature methods.<sup>11–13</sup> All reactions were done at room temperature.

**Reaction between K<sub>2</sub>[Fe<sup>II</sup>H<sub>3</sub>1(OH)] and *N*-Oxyl-2,2,6,6-tetramethylpiperidine (TEMPO).** K<sub>2</sub>[Fe<sup>II</sup>(H<sub>3</sub>1(OH))·2DMA (0.150 g, 0.196 mmol) in ~7 mL of dimethylacetamide (DMA) was reacted with TEMPO (0.031 g, 0.20 mmol), which was added in one portion as a solid. An immediate color change occurred from pale yellow to deep orange. After the mixture was stirred for 2 h at room temperature, crude compound was isolated after solvent removal under reduced pressure, followed by washing with diethyl ether and drying under vacuum. This compound was recrystallized after diffusing diethyl ether to DMA solution of the crude salt to produce K<sub>2</sub>[Fe<sup>III</sup>H<sub>3</sub>1(O)] in 63% yield (0.095 g). TEMPO–H was identified and quantified (75% yield) as the other product by gas chromatography.

**Reaction between K<sub>2</sub>[Mn<sup>III</sup>(H<sub>3</sub>1(O)) and *N*-Hydroxy-2,2,6,6-tetramethylpiperidine (TEMPO–H).** A 5 mL DMA solution of K<sub>2</sub>[Mn<sup>III</sup>H<sub>3</sub>1(O)]·2DMA (0.120 g, 0.157 mmol) was treated with TEMPO–H (0.027 g, 0.17 mmol) which was added at once as an oil. The reaction mixture turned from purplish-brown to deep yellow in color. After the mixture was stirred for 2 h at room temperature, solvent was removed under reduced pressure and the resulting solid was washed with pentane to obtain a pale yellow solid, which was recrystallized from DMA and diethyl ether to afford K<sub>2</sub>[Mn<sup>III</sup>H<sub>3</sub>1(OH)] (0.085 g, 71%). The pentane washings were combined and concentrated to produce the TEMPO radical in greater than 90% yield. The spectroscopic properties of these products match those previously reported of commercially obtained TEMPO and K<sub>2</sub>[Mn<sup>III</sup>H<sub>3</sub>1(OH)]<sup>11</sup> prepared by literature methods.

**Reaction of K<sub>2</sub>[M<sup>III</sup>H<sub>3</sub>1(O)] ( $M^{\text{III}} = \text{Mn}, \text{Fe}$ ) with 1,4-Cyclohexadiene (CHD).** K<sub>2</sub>[Mn<sup>III</sup>H<sub>3</sub>1(O)]·2DMA (0.15 g, 0.20 mmol) was dissolved in 10 mL of DMA. CHD (0.008 g, 0.098 mmol) was added, and the resulting solution stirred for 12 h at room temperature. During this time, the color of the solution changed from purplish-brown to faint yellow. A 2 mL aliquot was removed from the reaction mixture, diluted with 3 mL of diethyl ether, and passed through a short flash silica gel column. The ether-soluble product was determined to be benzene by gas chromatography (GC) in a yield of ~80%. The resultant metal salt was isolated from the reaction by removal of volatiles under reduced pressure. The residue was washed with diethyl ether and filtered. The isolated solid was washed again with ether and dried in vacuo to yield 0.145 g (95% yield). A similar procedure was carried out for Fe<sup>III</sup>–O with the following modifications: K<sub>2</sub>[Fe<sup>III</sup>H<sub>3</sub>1(O)]·2DMA (0.18 g, 0.24 mmol) and CHD (0.094 g, 1.180 mmol) were allowed to stir in 6 mL of DMA for 36 h at room temperature. K<sub>2</sub>[Fe<sup>II</sup>H<sub>3</sub>1(OH)] was isolated in 92% yield, while benzene was determined in 70% yield by gas chromatography. The spectroscopic properties for the isolated metal salts were identical to those already reported for K<sub>2</sub>[M<sup>III</sup>H<sub>3</sub>1(OH)].<sup>12</sup>

(13) Bordwell, F. G.; Liu, W.-Z. *J. Am. Chem. Soc.* **1996**, *118*, 10819–10823.

- (7) The BDE values are enthalpic quantities, and as Mayer points out,<sup>6e</sup> it is reasonable to assume that in our systems the entropy change is insignificant because the molecules involved are relatively large and differ only by a hydrogen atom.
- (8) (a) Baldwin, M. J.; Pecoraro, V. L. *J. Am. Chem. Soc.* **1996**, *118*, 11325–11326. (b) See ref 6c.
- (9) Caudle, M. T.; Pecoraro, V. L. *J. Am. Chem. Soc.* **1997**, *119*, 3415–3416.
- (10) (a) Jonas, R. T.; Stack, T. D. P. *J. Am. Chem. Soc.* **1997**, *119*, 8566–8567. (b) Goldsmith, C. R.; Jonas, R. T.; Stack, T. D. P. *J. Am. Chem. Soc.* **2002**, *124*, 83–96.
- (11) Gupta, R.; MacBeth, C. E.; Young, V. G., Jr.; Borovik, A. S. *J. Am. Chem. Soc.* **2002**, *124*, 1136–1137.
- (12) (a) Hammes, B. S.; Young, V. G., Jr.; Borovik, A. S. *Angew. Chem., Int. Ed.* **1999**, *38*, 666–669. (b) Shirin, Z.; Hammes, B. S.; Young, V. G., Jr.; Borovik, A. S. *J. Am. Chem. Soc.* **2000**, *122*, 1836–1837. (c) MacBeth, C. E.; Golombek, A. P.; Young, V. G., Jr.; Yang, C.; Kuczera, K.; Hendrich, M. P.; Borovik, A. S. *Science*, **2000**, *289*, 938–941. (d) MacBeth, C. E.; Hammes, B. S.; Young, V. G., Jr.; Borovik, A. S. *Inorg. Chem.* **2001**, *40*, 4733–4741.

**Reaction of  $K_2[M^{III}H_3I(O)]$  ( $M^{III} = Mn, Fe$ ) with 9,10-Dihydroanthracene (DHA).**  $K_2[Mn^{III}H_3I(O)] \cdot 2DMA$  (0.15 g, 0.20 mmol) was dissolved in  $\sim 10$  mL of DMA under an argon atmosphere. DHA (0.018 g, 0.098 mmol) was added in one portion, and the resulting solution was stirred for 2 h at room temperature. During this time period, the color of the solution changed from purplish-brown to faint pinkish-brown. Volatiles were removed under reduced pressure, and the organic compounds were removed with diethyl ether ( $6 \times 5$  mL). The ether layers were combined and passed through a short silica gel column, and the solvent was removed under reduced pressure to afford an off-white solid in 90% yield (0.016 g). This solid was confirmed to be anthracene by  $^1H$  NMR spectroscopy (in  $CDCl_3$ ) and gas chromatography (in diethyl ether). The metal salt was isolated from the remaining reaction mixture by filtration of an ether suspension. The solid was washed with ether and dried in vacuo. This solid,  $K_2[Mn^{III}H_3I(OH)]$ , was recrystallized by vapor diffusion of ether into a DMA solution of the solid; the yield was 90% (0.14 g). The reaction for the iron complex utilizes  $K_2[Fe^{III}H_3I(O)] \cdot 2DMA$  (0.18 g, 0.24 mmol) and DHA (0.213 g, 1.180 mmol) in 6 mL of DMA and was stirred for 36 h at room temperature. Both  $K_2[Fe^{III}H_3I(OH)]$  and anthracene were isolated in  $\sim 85\%$  yield. The FTIR and EPR properties of the final metal salts were identical to those reported for  $K_2[M^{III}H_3I(OH)]$ .<sup>12</sup>

**Reaction of  $K_2[M^{III}H_3I(O)]$  ( $M^{III} = Mn, Fe$ ) with 1,2-Diphenylhydrazine (DPH).** This reaction was done in a similar manner as that for DHA. The organic product was isolated in  $\sim 90\%$  yield and was characterized to be azobenzene after gas chromatographic and  $^1H$  NMR analysis. The metal compound was isolated in  $\sim 80$ – $90\%$  yield as  $K_2[M^{III}H_3I(OH)]$ , which was identified and characterized by EPR and FTIR spectroscopies.

**Reaction of  $K_2[Mn^{III}H_3I(O)]$  with Triphenylmethane (TPM), Diphenylmethane (DPM), Ethyl Benzene (EB), and 2,3-Dimethyl-2-butene (DMB).** In a typical experiment,  $K_2[Mn^{III}H_3I(O)] \cdot 2DMA$  (0.150 g, 0.196 mmol) was dissolved in 8 mL of DMA under an argon atmosphere, and an equimolar amount of the corresponding substrate was added. The mixture was allowed to stir for 6–12 h at room temperature. The color of the reaction mixture did not change during this time period. Volatiles were removed under reduced pressure, and the residue was washed several times with diethyl ether. The ether portions were combined, passed through a short silica gel column, and concentrated to dryness under reduced pressure. The mass of the resultant solid was  $\sim 90\%$  of the initial mass of the organic substrate. NMR spectroscopy and GC analysis were used to confirm the identity of these compounds as the unreacted organic substrates. The metal salt was isolated from the remaining reaction mixture by filtration from an ether suspension. The solid was washed with ether and dried in vacuo. This solid,  $K_2[Mn^{III}H_3I(O)]$ , was recrystallized by vapor diffusion of ether into a DMA solution of the solid; the yield was  $\sim 90\%$ . FTIR and UV–visible electronic spectroscopies confirmed the identity of this solid as  $K_2[Mn^{III}H_3I(O)]$ .

**Reaction of  $K_2[Mn^{III}H_3I(O)]$  with  $K_2[Fe^{III}H_3I(OH)]$ .**  $K_2[Mn^{III}H_3I(O)] \cdot 2DMA$  (0.105 g, 0.138 mmol) in 5 mL of DMA was treated with solid  $K_2[Fe^{III}H_3I(OH)] \cdot 2DMA$  (0.106 g, 0.138 mmol) under an argon atmosphere. An immediate color change was observed from purplish-brown to deep orange. After the mixture was stirred for 1 h, volatiles were removed under reduced pressure, and the resulting solid was washed with diethyl ether and dried under vacuum. The resulting solid was a mixture of  $K_2[Fe^{III}H_3I(O)]$  and  $K_2[Mn^{III}H_3I(OH)]$ , which could not be separated. However, spectroscopic characterization indicates that complete conversion to  $[Fe^{III}H_3I(O)]^{2-}$  and  $[Mn^{III}H_3I(OH)]^{2-}$  occurred. For  $[Fe^{III}H_3I(O)]^{2-}$ , the spectral data include EPR,  $g = 6.1$ ; FTIR (Nujol,  $cm^{-1}$ ),  $\nu(Fe-O) = 672$   $cm^{-1}$ ; and UV–vis (DMSO),  $\lambda = 330$  nm. For  $[Mn^{III}H_3I(OH)]^{2-}$  the spectral data include EPR, a broad signal at  $g \approx 2$  and FTIR (Nujol,  $cm^{-1}$ ),  $\nu(O-H) = 3654$   $cm^{-1}$ . In addition, the characteristic optical and FTIR features of  $[Mn^{III}H_3I(O)]^{2-}$  are absent.<sup>12</sup>

**Reaction of  $K_2[M^{III}H_3I(OH)]$  with  $KO_2$ .**  $K_2[M^{III}H_3I(OH)] \cdot 2DMA$

(0.18 g, 0.24 mmol) was dissolved in  $\sim 10$  mL of DMA under an argon atmosphere. Finely powdered  $KO_2$  (0.022 g, 0.31 mmol) was added in one portion as a solid, and the reaction mixture was stirred overnight, during which time the color of the reaction mixture changed to purplish-brown (manganese system) or deep yellow-orange (iron system). The mixtures were filtered, and the filtrate was dried under reduced pressure. Recrystallization was achieved by diffusing diethyl ether into a DMA solution of the crude product, to give yields of pure  $K_2[M^{III}H_3I(O)] \cdot 2DMA$  in yields ranging from 55 to 65%. The spectroscopic properties of the  $M^{III}-O$  products match those previously reported for  $[M^{III}H_3I(O)]^{2-}$ .<sup>12</sup> The reaction between  $K_2[M^{III}(H_3I)(^{18}OH)]$  (synthesized using  $H_2^{18}O$ ) and  $KO_2$  followed the same procedure and resulted in the formation of  $K_2[M^{III}H_3I(^{18}O)]$ . FTIR (Nujol,  $cm^{-1}$ ):  $\nu(Mn^{III}-^{18}O) = 672$ .

**Reaction of  $K_2[M^{III}H_3I(O)]$  with Substituted Phenols.** In a typical reaction,  $K_2[M^{III}H_3I(O)] \cdot 2DMA$  (0.085 g, 0.11 mmol) was dissolved in 8 mL of DMA and treated with solid 2,4,6-tri-*tert*-butylphenol (0.029 g, 0.11 mmol) under an argon atmosphere. The solution immediately changed color from purplish-brown to intense green (manganese system) and deep yellow-orange to red (iron system). After the solution was stirred for 2 h, the solvent was removed under reduced pressure and the solid was washed with diethyl ether.  $K[M^{III}H_3I(OH)]$  was isolated by filtration, washed with diethyl ether, and dried in vacuo to yield 0.078 g (95%) of the  $M^{III}-OH$  salt. Spectroscopic properties of the  $M^{III}-OH$  products were identical to those previously obtained for the  $K[M^{III}H_3I(OH)]$  complexes.<sup>12</sup> The conversion of  $[M^{III}H_3I(O)]^{2-}$  to  $[M^{III}H_3I(OH)]^{-}$  with phenol and 4-methoxyphenol was monitored with either optical (for  $[Mn^{III}H_3I(O)]^{2-}$ ) or EPR (for  $[Fe^{III}H_3I(O)]^{2-}$ ) spectroscopy.

**Reaction of  $K[M^{III}(H_3I)(OH)]$  with KOMe or KO<sup>t</sup>Bu.**  $K[Mn^{III}(H_3I)(OH)]$  (0.12 g, 0.22 mmol) was dissolved in 7 mL of DMA and treated with solid KOMe (0.018 g, 0.26 mmol) under an argon atmosphere. An immediate color change occurred from green to purplish-brown. The solution was stirred for 1 h. The filtrate was layered with diethyl ether, and microcrystalline  $K_2[Mn^{III}(H_3I)(O)]$  was obtained. An isolated yield of 55% (0.090 g) of  $K_2[Mn^{III}(H_3I)(O)]$  was obtained after filtration, washing with diethyl ether, and drying in vacuo. Deep yellow crystalline compound ( $K_2[Fe^{III}(H_3I)(O)]$ ) was isolated after the reaction between  $K[Fe^{III}(H_3I)(OH)]$  (0.15 g, 0.27 mmol) and KO<sup>t</sup>Bu (0.032 g, 0.280 mmol) in 60% yield following a similar method as discussed above. Spectroscopic properties for the metal salts were identical to those for pure samples of  $K_2[M^{III}(H_3I)(O)]$ .<sup>12</sup>

**Determination of  $pK_a$  Values for the Hydroxo Ligands ( $pK_a(M-OH)$ ) in  $[Mn^{III}H_3I(OH)]^{-}$  and  $[Fe^{III}H_3I(OH)]^{-}$ .** The  $pK_a(M-OH)$  value for  $[Mn^{III}H_3I(OH)]^{-}$  was obtained in DMSO using optical methods. The initial conversion of  $[Mn^{III}H_3I(O)]^{2-}$  to  $[Mn^{III}H_3I(OH)]^{-}$  was probed with a series of weak organic acids that have  $pK_a$  values ranging from 20 to 30.<sup>14</sup> These experiments set a range of 26.5 to 29.0  $pK_a$  units for the  $pK_a(M-OH)$  value in  $[Mn^{III}H_3I(OH)]^{-}$ . Spectrophotometric titrations were then performed with 4-aminopyridine ( $pK_a = 26.5$  in DMSO) and  $[Mn^{III}H_3I(O)]^{2-}$ . In a typical experiment,  $\sim 2.5$  mL of a 2–3 mM solution of  $K_2[Mn^{III}H_3I(O)] \cdot 2DMA$  in DMSO was titrated with a 1.5 M DMSO solution of 4-aminopyridine, which was added in aliquots varying from 0.005 to 0.015 mL. An absorbance spectrum was recorded after each addition. The  $pK_a(M-OH)$  was determined using the program SPECTFIT.<sup>15</sup> A two ligand, one metal ion model was used for the spectral analyses, where the first and second ligands were the conjugated base of 4-aminopyridine and  $[Mn^{III}H_3I(O)]^{2-}$ , respectively, and the metal ion was represented by a proton. The  $pK_a$  value for 4-aminopyridine was fixed at 26.5, while that for  $[Mn^{III}H_3I(OH)]^{-}$  was calculated using a nonlinear least-squares fit. The model used in the analysis is supported by the calculated initial and final

(14) Bordwell, F. G. *Acc. Chem. Res.* **1988**, *21*, 456–463.

(15) Binstead, R. A.; Zuberbuhler, A. D. *Spectfit*; Spectrum Associates: Chapel Hill, NC, 1993–97.



spectra, which correspond to that of [Mn<sup>III</sup>H<sub>3</sub>I(O)]<sup>2-</sup> and [Mn<sup>III</sup>H<sub>3</sub>I(OH)]<sup>-</sup> (Figure S1, Supporting Information).

The p*K*<sub>a</sub>(M–OH) value in DMSO for [Fe<sup>III</sup>H<sub>3</sub>I(OH)]<sup>-</sup> was done in a related manner, with the following modifications. The conversion of [Fe<sup>III</sup>H<sub>3</sub>I(O)]<sup>2-</sup> to [Fe<sup>III</sup>H<sub>3</sub>I(OH)]<sup>-</sup> was monitored using EPR spectroscopy and spectra were recorded at 77 K. A p*K*<sub>a</sub>(M–OH) range of 23.0 to 26.5 was determined initially, after which an EPR spectral titration was performed using 30–35 mM solutions of K<sub>2</sub>[Fe<sup>III</sup>H<sub>3</sub>I(O)] and 0.8–1.0 M solutions of diphenylamine (p*K*<sub>a</sub> = 24.95 in DMSO). This model also was able to calculate the initial and final EPR spectra from the titration experiment (Figure S2).

**Electrochemical Measurements.** Cyclic voltammetric experiments were conducted using a BAS CV 50W (Bioanalytical Systems Inc., West Lafayette, IN) voltammetric analyzer following methods previously described.<sup>16</sup> Anhydrous DMSO was obtained from Aldrich Chemical Co. and used without further purification. A 1.0 mm platinum electrode was used as the working electrode to measure the cyclic voltammograms (CV) for the [M<sup>III</sup>H<sub>3</sub>I(OH)]<sup>1-</sup>/[M<sup>III</sup>H<sub>3</sub>I(OH)]<sup>2-</sup> and [M<sup>III</sup>H<sub>3</sub>I(O)]<sup>2-</sup>/[M<sup>IV</sup>H<sub>3</sub>I(O)]<sup>-</sup> couples at scan velocities between 0.1 and 1.0 V s<sup>-1</sup>. A ferrocenium/ferrocene couple (Fc<sup>+0</sup>) was used to monitor the reference electrode (Ag<sup>+</sup>/Ag) and was observed at *E*<sub>1/2</sub> = 0.19 V with Δ*E*<sub>p</sub> = 0.115 V and *i*<sub>pa</sub>/*i*<sub>pc</sub><sup>-1</sup> = 0.85 at a *v* = 0.1 V s<sup>-1</sup> in DMSO under ambient temperature. The cyclic voltammograms for the [M<sup>IV</sup>H<sub>3</sub>I(O)]<sup>-</sup>/[M<sup>III</sup>H<sub>3</sub>I(O)]<sup>2-</sup> couples were also measured with a home-built 50 μm platinum electrode at a scan velocity of 50 V s<sup>-1</sup>. The performance of this system was also monitored with the Fc<sup>+0</sup> couple, which was found at an *E*<sub>1/2</sub> = 0.17 V versus Ag<sup>+</sup>/Ag, with a Δ*E*<sub>p</sub> = 0.100 V, and *i*<sub>pa</sub>/*i*<sub>pc</sub><sup>-1</sup> = 0.81. IR compensation was achieved before each CV was recorded. Redox potentials are reported versus the ferrocenium/ferrocene couple.

**Physical Measurements.** Electronic spectra were recorded with a Cary 50 spectrophotometer. X-band EPR spectra were collected using a Bruker EMX spectrometer equipped with an ER041XG microwave bridge. Spectra for all EPR samples were collected using the following spectrometer settings: attenuation = 15 dB, microwave power = 0.63 mW, frequency = 9.3 GHz, sweep width = 5000 G, modulation amplitude = 10.02 G, gain = 3.56 × 10<sup>-3</sup>, conversion time = 81.920 ms, time constant = 655.36 ms, and resolution = 1024 points. A quartz liquid nitrogen finger-dewar (Wilma Glass) was used to record spectra at 77 K. Gas chromatography was done on a Hewlett-Packard 6890 Series gas chromatograph equipped with an HP 7683 Series injector. A calibration plot was established for the quantitative determination of benzene and TEMPO–H using standard procedures.<sup>17</sup> The conductivities of DMSO solutions of K<sub>2</sub>[M<sup>III</sup>H<sub>3</sub>I(O)] and K[M<sup>III</sup>H<sub>3</sub>I(OH)] were measured using a YSI Model 35 conductance meter (YSI Scientific) and were K<sub>2</sub>[Fe<sup>III</sup>H<sub>3</sub>I(O)], 42 mho cm<sup>2</sup> mol<sup>-1</sup>; K<sub>2</sub>[Mn<sup>III</sup>H<sub>3</sub>I(O)], 40 mho cm<sup>2</sup> mol<sup>-1</sup>; K[Fe<sup>III</sup>H<sub>3</sub>I(OH)], 23 mho cm<sup>2</sup> mol<sup>-1</sup>; K[Mn<sup>III</sup>H<sub>3</sub>I(OH)], 25 mho cm<sup>2</sup> mol<sup>-1</sup>. Standards: <sup>n</sup>Bu<sub>4</sub>NCl, 24 mho cm<sup>2</sup> mol<sup>-1</sup>; K<sub>2</sub>Cr<sub>2</sub>O<sub>7</sub>, 37 mho cm<sup>2</sup> mol<sup>-1</sup>; Zn(ClO<sub>4</sub>)<sub>2</sub>·H<sub>2</sub>O, 38 mho cm<sup>2</sup> mol<sup>-1</sup>; [Fe(dmsO)<sub>6</sub>](ClO<sub>4</sub>)<sub>3</sub>, 70 mho cm<sup>2</sup> mol<sup>-1</sup>.

## Results and Discussion

The [M<sup>III</sup>H<sub>3</sub>I(OH)]<sup>2-</sup> (M<sup>II</sup> = Mn, Fe) complexes were prepared using water as the source of the hydroxo ligands. The hydroxo and oxo ligands in the [M<sup>III</sup>H<sub>3</sub>I(OH)]<sup>-</sup> and [M<sup>III</sup>H<sub>3</sub>I(O)]<sup>2-</sup> complexes (M<sup>III</sup> = Mn, Fe) were derived from either dioxygen or water. Details of their preparation have been reported.<sup>11,12</sup> These complexes are stable in DMSO, which was the solvent used in all the following studies. Conductivity measurements done in DMSO indicated that K<sub>2</sub>[M<sup>III</sup>H<sub>3</sub>I(O)] are 2:1 electrolytes, while the K[M<sup>III</sup>H<sub>3</sub>I(OH)] salts are 1:1 electrolytes.

(16) Ray, M.; Hammes, B. S.; Yap, G. P. A.; Rheingold, A. H.; Liable-Sands, L.; Borovik, A. S. *Inorg. Chem.* **1998**, *37*, 1527–1532.

(17) Landgrebe, J. A. *Organic Laboratory*, 4th ed.; Brooks/Cole: Pacific Grove, CA, 1993.

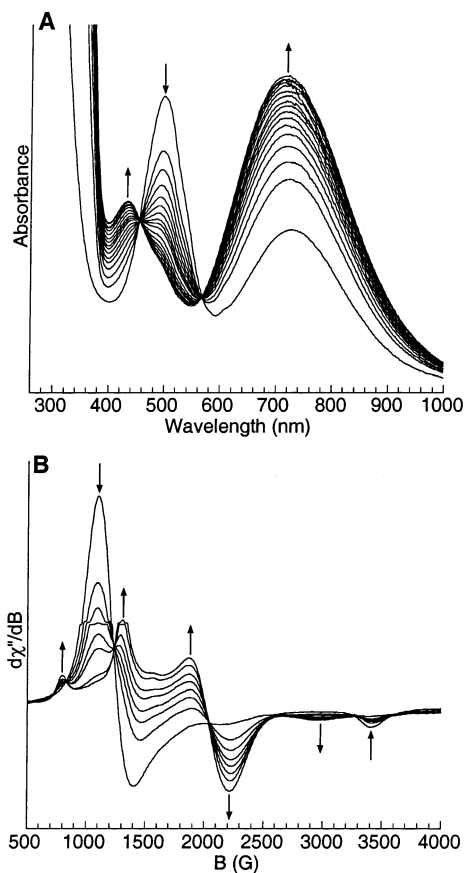


**Figure 1.** Titration of [Mn<sup>III</sup>H<sub>3</sub>I(O)]<sup>2-</sup> with 4-aminopyridine (A) measured by absorbance spectroscopy and [Fe<sup>III</sup>H<sub>3</sub>I(O)]<sup>2-</sup> with diphenylamine (B) followed by EPR spectroscopy. All titrations were done in DMSO.

The M<sup>III</sup>–OH and M<sup>III</sup>–O complexes have trigonal bipyramidal coordination geometry, where the three-deprotonated urea nitrogens define the basal plane and the oxo or hydroxo oxygen donors are trans to the apical nitrogen atom. The M–O(H) units are confined within a cavity provided by the remaining components of the [H<sub>3</sub>I]<sup>3-</sup> ligand. The resultant cavity structure disposes three hydrogen bond donors inward toward the M–O(H) units, which form intramolecular H-bonds with the oxo or hydroxo ligands. These complexes thus provide the first opportunity to evaluate p*K*<sub>a</sub>(M–OH), redox, and BDE<sub>O–H</sub> properties of M–O(H) complexes having the same primary and secondary coordination spheres.<sup>18</sup>

**p*K*<sub>a</sub>(M–OH) Values for [Mn<sup>III</sup>H<sub>3</sub>I(OH)]<sup>-</sup> and [Fe<sup>III</sup>H<sub>3</sub>I(OH)]<sup>-</sup>.** Figure 1A shows the electronic absorbance spectra obtained for the titration of [Mn<sup>III</sup>H<sub>3</sub>I(O)]<sup>2-</sup> with 4-aminopyridine in DMSO. Clean conversion to the [Mn<sup>III</sup>H<sub>3</sub>I(OH)]<sup>-</sup> complex is observed with isobestic points at 455 and 566 nm. A p*K*<sub>a</sub>(Mn<sup>III</sup>–OH) of 28.3(1) was determined from the analysis of these data (see Experimental Section). Similar titration experiments and analysis were performed in DMSO for [Fe<sup>III</sup>H<sub>3</sub>I(OH)]<sup>-</sup>, which yielded a p*K*<sub>a</sub>(Fe<sup>III</sup>–OH) of 25.0(1).

(18) For discussions on the effects of the secondary coordination, particularly those of hydrogen bonds, on the function of active sites in protein, see: (a) Ozaki, S.; Roach, M. P.; Matsui, T.; Watanabe, Y. *Acc. Chem. Res.* **2001**, *34*, 818–825. (b) Yikilmaz, E.; Xie, J.; Brunold, T. C.; Miller, A.-F. *J. Am. Chem. Soc.* **2002**, *124*, 3482–3483. (c) Xie, J.; Yikilmaz, E.; Miller, A.-F.; Brunold, T. C. *J. Am. Chem. Soc.* **2002**, *124*, 3769–3774. (d) Maliekal, J.; Karapetian, A.; Vance, C.; Yikilmaz, E.; Wu, Q.; Jackson, T.; Brunold, T. C.; Spiro, T. G.; Miller, A.-F. *J. Am. Chem. Soc.* **2002**, *124*, 15064–15075. (e) Jackson, T. A.; Xie, J.; Yikilmaz, E.; Miller, A.-F.; Brunold, T. C. *J. Am. Chem. Soc.* **2002**, *124*, 10833–10845.

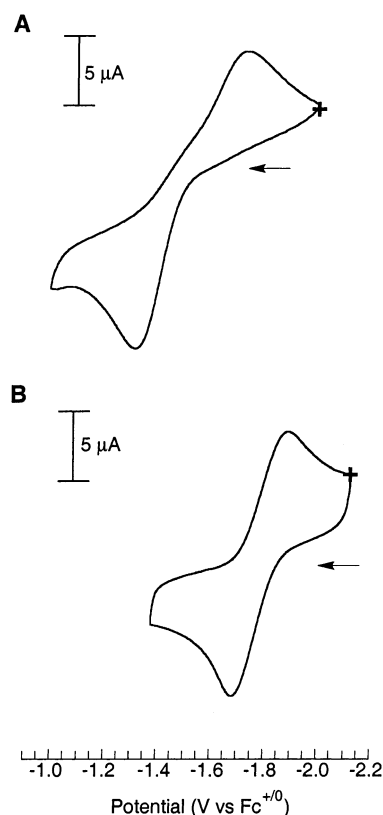


**Figure 2.** Cyclic voltammograms of  $[\text{Mn}^{\text{III}}\text{H}_3\text{I}(\text{OH})]^{2-}$  (A) and  $[\text{Mn}^{\text{III}}\text{H}_3\text{I}(\text{OH})]^{2-}$  (B) recorded in DMSO at a scan velocity of  $0.01 \text{ V s}^{-1}$ .

**Table 1.**  $\text{p}K_{\text{a}}(\text{M}-\text{OH})$  and Electrochemical Properties for the  $\text{M}-\text{O}(\text{H})$  Complexes<sup>a</sup>

complex	$\text{p}K_{\text{a}}(\text{M}-\text{OH})$	$E_{1/2}^b$ (V)	$\Delta E_p^b$ (V)	$i_{\text{pa}}/i_{\text{pc}}^{-1}$
$[\text{Mn}^{\text{III}}\text{H}_3\text{I}(\text{OH})]^-$	28.3(1)	-1.51	0.38	0.77
$[\text{Fe}^{\text{III}}\text{H}_3\text{I}(\text{OH})]^-$	25.0(1)	-1.79	0.19	0.71
$[\text{Mn}^{\text{III}}\text{H}_3\text{I}(\text{O})]^{2-}$		-0.076(-0.02) <sup>c</sup>	0.11	0.92
$[\text{Fe}^{\text{III}}\text{H}_3\text{I}(\text{O})]^{2-}$		0.34 <sup>c</sup>		

<sup>a</sup> In DMSO. <sup>b</sup> Versus  $\text{Fc}^{+/0}$  couple. <sup>c</sup> Irreversible process,  $E_{\text{a}}$  value measured at  $\nu = 0.1 \text{ V s}^{-1}$ .

EPR spectroscopy was used to monitor the conversion of  $[\text{Fe}^{\text{III}}\text{H}_3\text{I}(\text{O})]^{2-}$  to  $[\text{Fe}^{\text{III}}\text{H}_3\text{I}(\text{OH})]^-$ , as shown in Figure 1B using diphenylamine as the acid.

**Electrochemical Properties.** The CVs for the  $\text{M}^{\text{III/II}}-\text{OH}$  couples recorded in DMSO are shown in Figure 2. Both redox responses are quasi-reversible at scan rates between 0.1 and  $1.0 \text{ V s}^{-1}$  (Table 1). An  $E_{1/2} = -1.51 \text{ V}$  versus  $\text{Fc}^{+/0}$  was observed for the  $[\text{Mn}^{\text{III/II}}\text{H}_3\text{I}(\text{OH})]^{-/2-}$  couple, while the  $[\text{Fe}^{\text{III/II}}\text{H}_3\text{I}(\text{OH})]^{-/2-}$  potential is at  $-1.79 \text{ V}$  versus  $\text{Fc}^{+/0}$ ; this potential is similar to that reported for the  $[\text{Fe}^{\text{III/II}}\text{H}_3\text{I}(\text{OH})]^{-/2-}$  couple measured in DMF ( $E_{1/2} = -1.85 \text{ V}$  versus  $\text{Fc}^{+/0}$ ).<sup>12d,19</sup>

$[\text{Mn}^{\text{III}}\text{H}_3\text{I}(\text{O})]^{2-}$  and  $[\text{Fe}^{\text{III}}\text{H}_3\text{I}(\text{O})]^{2-}$  have irreversible oxidative processes at  $E_{\text{pa}}$  values of  $-0.022$  and  $0.34 \text{ V}$  versus  $\text{Fc}^{+/0}$  at scan velocities between 0.1 and  $10.0 \text{ V s}^{-1}$  (Figure 3). For  $[\text{Mn}^{\text{III}}\text{H}_3\text{I}(\text{O})]^{2-}$ , this oxidative process became reversible, with an  $E_{1/2}$  of  $-0.076 \text{ V}$  versus  $\text{Fc}^{+/0}$ , at the faster scan velocity of  $50 \text{ V s}^{-1}$  (Figure 3A, Table 1).<sup>20</sup> Note, however, that an increase

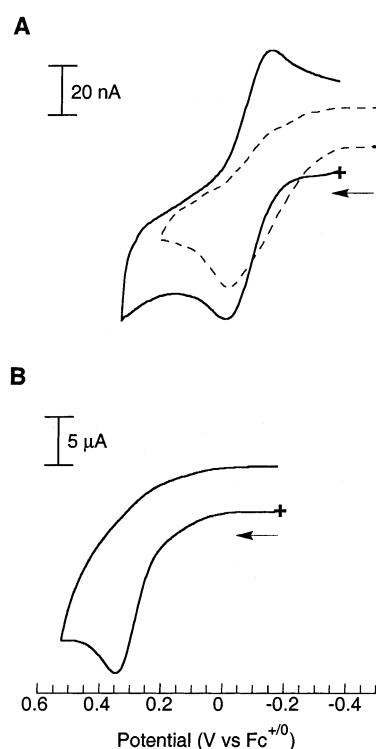


**Figure 3.** Cyclic voltammograms of  $[\text{Mn}^{\text{III}}\text{H}_3\text{I}(\text{O})]^{2-}$  (A) measured at a scan velocity of  $50 \text{ V s}^{-1}$  (—) and  $0.1 \text{ V s}^{-1}$  (---) and  $[\text{Fe}^{\text{III}}\text{H}_3\text{I}(\text{O})]^{2-}$  (B) measured at  $0.1 \text{ V s}^{-1}$ . All measurements were made in DMSO.

in the scan velocity did not alter the CV for  $[\text{Fe}^{\text{III}}\text{H}_3\text{I}(\text{O})]^{2-}$  from those recorded at slower rates. These redox features are assigned to the one-electron oxidation of the  $\text{M}^{\text{III}}-\text{O}$  complexes, to formally yield the  $\text{M}^{\text{IV}}-\text{oxo}$  species, which are unstable in DMSO at ambient temperature and scan velocities between 0.1 and  $40 \text{ V s}^{-1}$ .  $[\text{Mn}^{\text{IV}}\text{H}_3\text{I}(\text{O})]^-$  appears to be stable at the relatively fast scan velocity of  $50 \text{ V s}^{-1}$ , while the related  $\text{Fe}^{\text{IV}}-\text{oxo}$  complex is still too unstable to be observed on this time scale.

**Evaluation of the  $\text{BDE}_{\text{O}-\text{H}}$  for  $[\text{Mn}^{\text{III}}\text{H}_3\text{I}(\text{OH})]^-$  and  $[\text{Fe}^{\text{III}}\text{H}_3\text{I}(\text{OH})]^-$ .** The extensive writings of Mayer<sup>6</sup> have illustrated that the homolytic  $\text{BDE}_{\text{O}-\text{H}}$  of manganese complexes can be determined from eq 1.

$$\text{BDE}_{\text{O}-\text{H}} = 23.06E_{1/2} + 1.37\text{p}K_{\text{a}} + C \quad (1)$$

His approach is adapted from the methods developed by Bordwell and Tilset for determining  $\text{BDE}_{\text{S}-\text{H}}$  of organic compounds in condensed phases.<sup>21</sup> Equation 1 shows that the  $\text{BDE}_{\text{O}-\text{H}}$  calculations involve independent energy measurements for electron ( $E_{1/2}$  values) and proton ( $\text{p}K_{\text{a}}$  values) transfers and can be expressed in thermodynamic cycles as shown in Figure 4. The constant,  $C$ , is also included in eq 1 to account for the thermodynamic properties of the hydrogen atom in solution and is dependent on solvent and the reference electrode used to measure the redox potentials. Our calculations used  $C = 73.3 \text{ kcal/mol}$ , the value determined previously for DMSO and the  $\text{Fc}^{+/0}$  reference electrode.<sup>21</sup> An illustration of the calculations is shown in Scheme 1 for the  $\text{BDE}_{\text{O}-\text{H}}$  of  $[\text{Mn}^{\text{III}}\text{H}_3\text{I}(\text{O}-\text{H})]^{2-}$ ; the remaining calculations are in the Supporting Information.

(19) The potential for the normal hydrogen electrode versus  $\text{Fc}^{+/0}$  in DMSO is approximately  $-0.65 \text{ V}$ .

(20) The  $E_{\text{pa}}$  of the  $[\text{Mn}^{\text{IV}}\text{H}_3\text{I}(\text{O})]^-$  couple only changes by  $6 \text{ mV}$  ( $-0.016$  versus  $-0.022 \text{ mV}$ ) for the higher velocity CV compared to that measured at the scan velocity of  $0.1 \text{ V/s}$ .

(21) (a) Bordwell, F. G.; Cheng, J.-P.; Ji, G.-Z.; Satish, A. V.; Zhang, X. J. *Am. Chem. Soc.* **1991**, *113*, 9790–9795. (b) Parker, V. D.; Handoo, K. L.; Roness, F.; Tilset, M. *J. Am. Chem. Soc.* **1991**, *113*, 7493–7498.

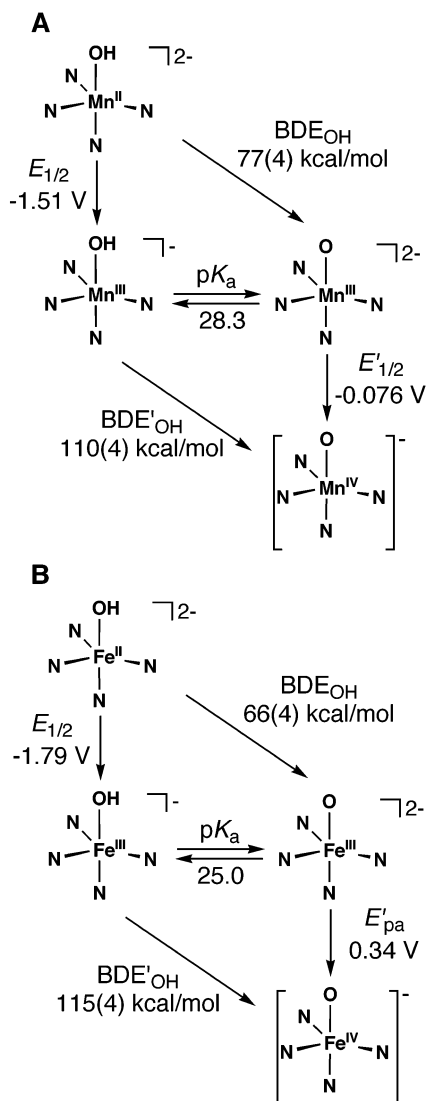


**Figure 4.** Thermodynamic cycles used to determine the  $BDE_{O-H}$  for  $[Mn^{III}H_3I(O-H)]^{2-}$  (A) and  $[Fe^{III}H_3I(O-H)]^{2-}$  (B).

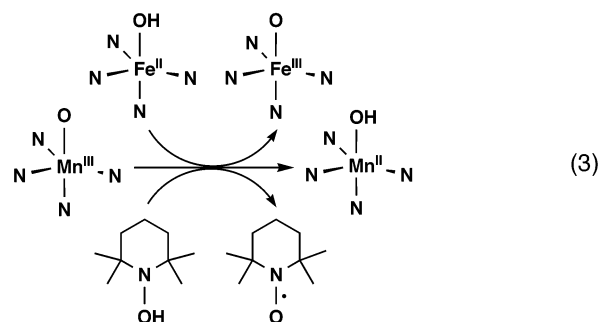
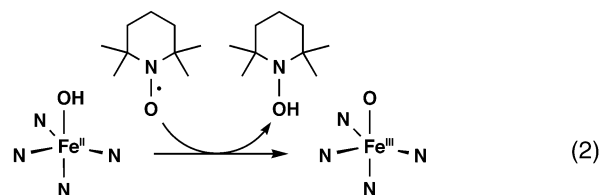
A  $BDE_{O-H}$  value of 77(4) kcal/mol was obtained for  $[Mn^{III}H_3I(O-H)]^{2-}$  using the above method and is within the range found for other mono- and binuclear manganese complexes. For instance,  $[Mn^{VI}O_3(O-H)]^-$  has a  $BDE_{O-H}$  of 83(4) kcal/mol, while those of the dimers  $[(phen)_2Mn^{IV}(\mu-O)(\mu-O-H)Mn^{III}(phen)_2]^{3+}$  and  $[Mn^{III}Mn^{IV}(\mu-O)(\mu-O-H)(salpn)_2]$  are 79 and 76 kcal/mol, respectively.<sup>22</sup>  $[Fe^{II}H_3I(O-H)]^{2-}$  has a  $BDE_{O-H}$  of 66(4) kcal/mol. The 11 kcal/mol difference in  $BDE_{O-H}$  between these two  $M^{II}-OH$  complexes is attributed, almost equally, to the lower  $pK_a$  and redox potential for the  $M^{III/II}-OH$  couple in  $[Fe^{III}H_3I(OH)]^-$  (Figure 4). We are unaware of reports on the  $BDE_{S_{O-H}}$  for other Fe-OH complexes; the only related studies are those of Stack for the ferrous water and methanol complexes,  $[Fe^{II}(H_2O)_5(HO-H)]^{2+}$  and  $[Fe^{II}(PY5)(MeO-H)]^{2+}$ , which have  $BDE_{S_{O-H}}$  of 77 and 84 kcal/mol, respectively.<sup>10</sup>

A  $BDE_{O-H} = 110(4)$  kcal/mol was determined for  $[Mn^{III}H_3I(O-H)]^-$ , a value that is significantly larger than those

calculated for other manganese complexes by this method (Table 2). The only comparable value is the  $BDE_{O-H}$  of 103 kcal/mol found for  $Mn^{III}(O-H)(OH)_2(H_2O)_2$ , which was determined from density functional theory.<sup>23</sup> This theoretical study suggests that monomeric  $Mn^{IV}$  species with a terminal oxo ligand has a large thermodynamic driving force for the transfer of hydrogen atoms, a proposal that is supported by our  $BDE_{O-H}$  results for  $[Mn^{III}H_3I(O-H)]^-$ . This affinity for H-atoms is the most likely cause for the instability of the one-electron oxidized product of  $[Mn^{III}H_3I(O)]^-$  generated electrochemically.

By a similar method, a  $BDE_{O-H}$  of 115(4) kcal/mol was found for  $[Fe^{III}H_3I(O-H)]^-$ ,<sup>24</sup> a value similar to that found for  $[Mn^{III}H_3I(O-H)]^-$ . These results also indicate that there is a large increase in the  $BDE_{S_{O-H}}$  between  $M^{II}-OH$  and  $M^{III}-OH$  complexes: a 49 kcal/mol increase in  $BDE_{O-H}$  is observed for the  $[Fe^{II}H_3I(OH)]^{2-}/[Fe^{III}H_3I(OH)]^-$  complexes, while the  $[Mn^{II}H_3I(OH)]^{2-}/[Mn^{III}H_3I(OH)]^-$  pair have a 33 kcal/mol difference. These changes in  $BDE_{S_{O-H}}$  are caused by the large increase in redox potentials of the  $[M^{IV/III}H_3I(O)]^{-/2-}$  process (vide supra). A greater than 2.0 V increase is observed for the oxidation of  $[Fe^{III}H_3I(O)]^-$  compared to that of  $[Fe^{II}H_3I(OH)]^{2-}$ , while, in the analogous manganese systems, the change is  $\sim 1.4$  V.

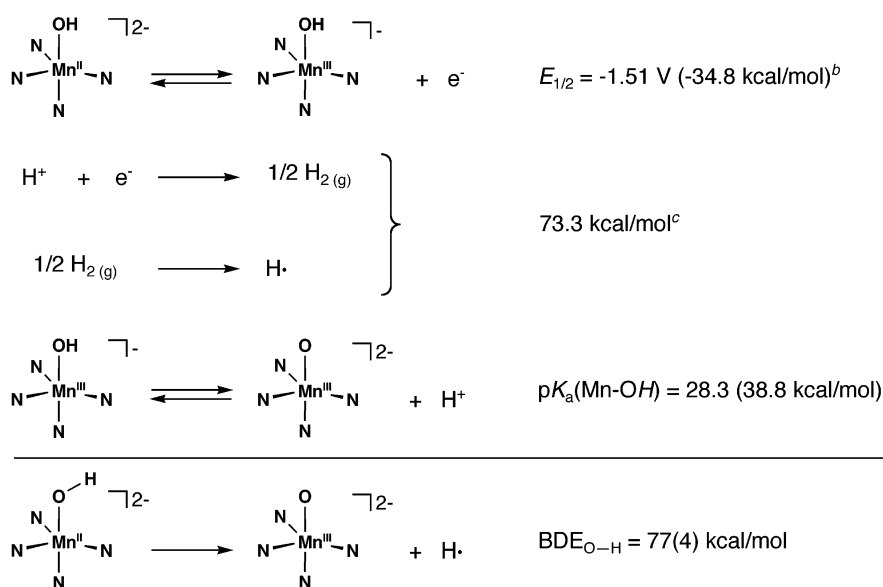
**Reactivity Studies. (A) Reactivity with O-H Substrates.** The experimentally determined  $BDE_{O-H}$  values for the  $M-OH$  complexes give us a thermodynamic basis for predicting the reactivity of these complexes, which can be verified through experimental studies. For instances, TEMPO-H has a  $BDE_{O-H}$  of 70 kcal/mol<sup>13</sup>, a value that is 4 kcal/mol larger than that found for  $[Fe^{II}H_3I(OH)]^{2-}$ . Therefore, treating  $[Fe^{II}H_3I(OH)]^{2-}$  with the TEMPO radical afforded  $[Fe^{III}H_3I(O)]^{2-}$  (60% recrystallized yield) and TEMPO-H (75% yield) as the only organic product (eq 2).<sup>25</sup> In contrast, no reaction was observed when  $[Mn^{II}H_3I(OH)]^{2-}$  was mixed with the TEMPO radical. A reaction did take place between TEMPO-H and  $[Mn^{III}H_3I(O)]^{2-}$ , producing  $[Mn^{II}H_3I(OH)]^{2-}$  (70% recrystallized yield) and the TEMPO radical (>90% yield) (eq 3), which was characterized by EPR and FTIR spectroscopies. These findings are consistent



$[Mn^{III}H_3I(O)]^{2-}$  was mixed with the TEMPO radical. A reaction did take place between TEMPO-H and  $[Mn^{III}H_3I(O)]^{2-}$ , producing  $[Mn^{II}H_3I(OH)]^{2-}$  (70% recrystallized yield) and the TEMPO radical (>90% yield) (eq 3), which was characterized by EPR and FTIR spectroscopies. These findings are consistent

(22) Ligand abbreviations: PY5, 2,6-bis-(2-pyridyl)methoxymethane)pyridine; salpn, 1,3-bis(salicylideneamino)propane; phen, 1,10-phenanthroline; bpy, bipyridine; L, 2-hydroxy-1,3-bis(3,5-X<sub>2</sub>-salicylideneamino)propane (X = Cl, H, di-*tert*-butyl).

(23) (a) Siegbahn, P. E. M. *Inorg. Chem.* **2000**, *39*, 2923–2935. (b) Blomberg, M. R. A.; Siegbahn, P. E. M. *Theor. Chem. Acc.* **1997**, *97*, 72–80.

Scheme 1<sup>a</sup>

<sup>a</sup> In DMSO. <sup>b</sup> Versus  $\text{Fc}^{+/0}$ . <sup>c</sup> From ref 19.

Table 2. Comparison of  $\text{BDE}_{\text{O-H}}$  Values<sup>a</sup>

complex	$\text{BDE}_{\text{O-H}}$ (kcal/mol)	ref
$\text{K}_2[\text{Mn}^{\text{II}}\text{H}_3\text{I}(\text{O}-\text{H})]$	77	this work
$\text{K}[\text{Mn}^{\text{III}}\text{H}_3\text{I}(\text{O}-\text{H})]$	110	this work
$[\text{Mn}^{\text{II}}(\text{H}_2\text{O})_5(\text{HO}-\text{H})]^{2-}$	90	this work
$\text{Mn}^{\text{III}}(\text{O}-\text{H})(\text{OH})_2(\text{H}_2\text{O})_2^b$	103	23
$[\text{H}-\text{OMn}^{\text{VI}}\text{O}_3]^-$	83	6a
$[(\text{phen})_2\text{Mn}^{\text{II}}(\mu-\text{O}-\text{H})_2\text{Mn}^{\text{III}}(\text{phen})_2](\text{PF}_6)_3$	75	6c
$[(\text{phen})_2\text{Mn}^{\text{III}}(\mu-\text{O})(\mu-\text{O}-\text{H})\text{Mn}^{\text{IV}}(\text{phen})_2](\text{PF}_6)_3$	79	6c
$[\text{Mn}^{\text{III}}\text{Mn}^{\text{IV}}(\mu-\text{O})(\mu-\text{O}-\text{H})(\text{salpn})_2]$	76	8a
$[\text{Mn}^{\text{III}}\text{Mn}^{\text{IV}}(\mu-\text{O})(\mu-\text{O}-\text{H})(\text{bpy})_2]^{4+}$	84	8a
$[\text{Mn}^{\text{III}}\text{L}_2(\text{OH}_2)]$	82–89	9
$[\text{Mn}^{\text{III}}\text{Mn}^{\text{IV}}\text{L}_2(\text{HO}-\text{H})]^+$	86–94	9
$[\text{Fe}^{\text{II}}(\text{PY5})(\text{MeO}-\text{H})(\text{OTf})_2]$	84	10
$[\text{Fe}^{\text{II}}(\text{H}_2\text{O})_5(\text{HO}-\text{H})]^{2+}$	77	10b
$\text{K}_2[\text{Fe}^{\text{II}}\text{H}_3\text{I}(\text{O}-\text{H})]$	66	this work
$\text{K}_2[\text{Fe}^{\text{III}}\text{H}_3\text{I}(\text{O}-\text{H})]^c$	115	this work

<sup>a</sup> For abbreviation, see ref 22. <sup>b</sup> Determined from density functional theory. <sup>c</sup> An upper limit; determined using  $E_{\text{pa}}$  for  $[\text{Fe}^{\text{III}}\text{H}_3\text{I}(\text{O})]^{2-}$ .

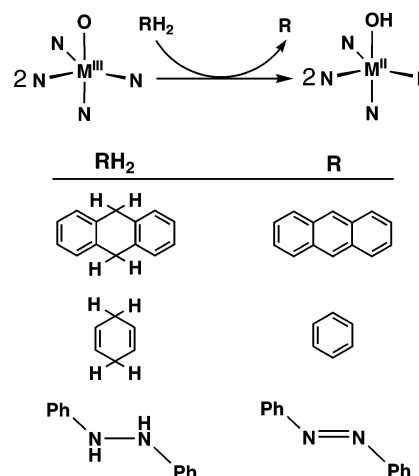
with  $[\text{Mn}^{\text{II}}\text{H}_3\text{I}(\text{OH})]^{2-}$  having a larger  $\text{BDE}_{\text{O-H}}$  compared to that of  $\text{TEMPO}-\text{H}$ .

$[\text{Mn}^{\text{II}}\text{H}_3\text{I}(\text{OH})]^{2-}$  and  $[\text{Fe}^{\text{II}}\text{H}_3\text{I}(\text{OH})]^{2-}$  also react with  $\text{KO}_2$  to yield their corresponding  $\text{M}^{\text{III}}-\text{O}$  complexes in recrystallized yields of 55–65%. While not isolated,  $\text{KO}_2\text{H}$  is proposed to be an initial product based on the known  $\text{BDE}_{\text{O-H}}$  of 90 kcal/mol for the related peroxide  $\text{H}_2\text{O}_2$ .<sup>26</sup> Isotopic labeling studies with  $[\text{Mn}^{\text{II}}\text{H}_3\text{I}(\text{OH})]^{2-}$  resulted in the formation of  $[\text{Mn}^{\text{III}}\text{H}_3\text{I}(\text{O})]^{2-}$  (characterized by FTIR spectroscopy), supporting the formal

(24) This calculation provides an upper limit for the  $\text{BDE}_{\text{O-H}}$  because only the  $E_{\text{pa}}$  could be measured for the  $[\text{Fe}^{\text{IV}}\text{H}_3\text{I}(\text{O})]^{2-}$  redox process. However, we do not believe that the  $\text{BDE}_{\text{O-H}}$  is significantly affected by the use of oxidative potential. In fact,  $E_{\text{pa}}$  values are often used in calculating bond dissociation energies when  $E_{1/2}$  values cannot be obtained. For example, Bordwell has used  $E_{\text{pa}}$  in his reports when the  $E_{1/2}$  is difficult to determine.<sup>21a</sup> His findings show that using  $E_{\text{pa}}$  is justified in calculating BDE, since plots of  $E_{1/2}$  (reversible) versus  $E_{\text{pz}}$  (irreversible) are linear. In addition, it was found that the reversible oxidation potentials for several anions, obtained using high-speed voltammetry, are nearly identical to those obtained for irreversible CV. Our results on  $[\text{Mn}^{\text{III}}(\text{H}_3\text{I})(\text{OH})]^-$  support these findings (Figure 3A). It has also been suggested that quasi-reversible couples cause a  $\pm 50$  mV change in potential, which has a small effect on the BDE.<sup>6c</sup>

(25) Determined by gas chromatography; see Experimental Section.

(26) *CRC Handbook of Chemistry and Physics*, 72nd ed.; Lide, D. R., Ed.; CRC Press: Boca Raton, FL, 1991; pp 9–115.

Chart 2. Reactivity of the  $\text{M}^{\text{III}}-\text{O}$  Complexes

transfer of a hydrogen atom. Further support for this type of process is provided by the reaction of  $[\text{Fe}^{\text{II}}\text{H}_3\text{I}(\text{OH})]^{2-}$  and  $[\text{Mn}^{\text{II}}\text{H}_3\text{I}(\text{O})]^{2-}$ , which produces  $[\text{Fe}^{\text{III}}\text{H}_3\text{I}(\text{O})]^{2-}$  and  $[\text{Mn}^{\text{II}}\text{H}_3\text{I}(\text{OH})]^{2-}$ . This reactivity is expected based on the 11 kcal/mol difference in  $\text{BDE}_{\text{O-H}}$  between the two  $\text{M}^{\text{II}}-\text{OH}$  complexes,  $[\text{Fe}^{\text{II}}\text{H}_3\text{I}(\text{OH})]^{2-}$  and  $[\text{Mn}^{\text{II}}\text{H}_3\text{I}(\text{OH})]^{2-}$  (Table 2).

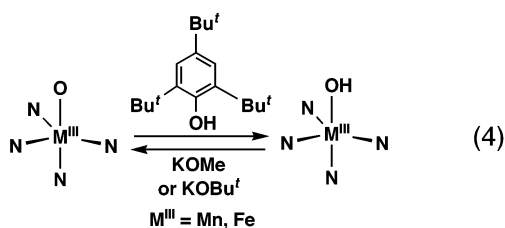
**(B) Reactivity of the  $\text{M}^{\text{III}}-\text{O}$  Complexes with Organic Substrates Containing X–H (X = C, N) Bonds.** The isolated manganese and iron  $\text{M}^{\text{III}}-\text{O}$  complexes were examined for their reactivity with organic substrates containing relatively weak X–H (where X = C or N) bonds (Chart 2). According to the BDE calculations,  $[\text{Mn}^{\text{III}}\text{H}_3\text{I}(\text{O})]^{2-}$  is capable of reacting with a substrate having an X–H bond strength of  $\sim 77$  kcal/mol. Therefore,  $[\text{Mn}^{\text{III}}\text{H}_3\text{I}(\text{O})]^{2-}$  was able to oxidize 9,10-dihydroanthracene (DHA,  $\text{BDE}_{\text{C-H}} \approx 78$  kcal/mol) to anthracene in 95% yield. The resultant metal complex was isolated in 90% yield and identified as  $[\text{Mn}^{\text{II}}\text{H}_3\text{I}(\text{OH})]^{2-}$ , the anticipated product for the transfer of a hydrogen atom. Note that none of the oxygen-containing organic products (e.g., anthraquinone or anthrone) were found in the gas chromatogram. The analogous reaction of  $[\text{Mn}^{\text{III}}\text{H}_3\text{I}(\text{O})]^{2-}$  with 1,4-cyclohexadiene (CHD,  $\text{BDE}_{\text{C-H}} \approx$



77 kcal/mol) also produced K<sub>2</sub>[Mn<sup>II</sup>(H<sub>3</sub>1)(OH)] (95% yield) and benzene (80% yield) as the only organic product. In addition, [Mn<sup>III</sup>H<sub>3</sub>1(O)]<sup>2-</sup> oxidizes 1,2-diphenylhydrazine (DPH) to azobenzene in nearly quantitative yield. Under similar experimental conditions, no reaction was observed when [Mn<sup>III</sup>H<sub>3</sub>1(O)]<sup>2-</sup> complex was treated with substrates having BDE<sub>C-H</sub> > 80 kcal/mol. These substrates include triphenylmethane (BDE<sub>C-H</sub> = 81 kcal/mol), diphenylmethane (BDE<sub>C-H</sub> = 82 kcal/mol), ethylbenzene (BDE<sub>C-H</sub> = 85 kcal/mol), 2,3-dimethyl-2-butene (BDE<sub>C-H</sub> = 84 kcal/mol), and toluene (BDE<sub>C-H</sub> = 89 kcal/mol). It is important to note that less than 5% yield of 1,1,2,2-tetraethylethane was observed after 24 h, when 10 equiv of diphenylmethane was used in the reaction with [Mn<sup>III</sup>H<sub>3</sub>1(O)]<sup>2-</sup>.

[Fe<sup>III</sup>H<sub>3</sub>1(O)]<sup>2-</sup> has similar reactivity with DHA, CHD, and DPH. In all these reactions, K<sub>2</sub>[Fe<sup>II</sup>(H<sub>3</sub>1)(OH)] was isolated in nearly quantitative amounts. Qualitatively, the reactions of the [Fe<sup>III</sup>H<sub>3</sub>1(O)]<sup>2-</sup> complex with these substrates were slower compared to those with [Mn<sup>III</sup>H<sub>3</sub>1(O)]<sup>2-</sup> and often required an excess (2–5 equiv) of the organic reactant for complete conversion to [Fe<sup>II</sup>H<sub>3</sub>1(OH)]<sup>2-</sup>. These observations are consistent with the fact that the manganese system has a larger driving force to form a O–H bond (vide supra), which would result in a greater rate.<sup>27</sup> Finally, the related M<sup>III</sup>–OH complexes, [Fe<sup>III</sup>H<sub>3</sub>1(OH)]<sup>-</sup> and [Mn<sup>III</sup>H<sub>3</sub>1(OH)]<sup>-</sup>, do not react with DHA, CHD, DPM, TPM, and DMB. No observable loss in the spectral features of the M<sup>III</sup>–OH complexes were found, even after prolonged stirring (48 h).

**(C) Reactivity of the M<sup>III</sup>–O Complexes with Phenolic Substrates.** 2,4,6-Tri-*tert*-butylphenol (TBP) has a BDE<sub>O-H</sub> of 81 kcal/mol<sup>28</sup> and is often used as a substrate in a hydrogen atom transfer reaction because it forms a stable phenoxyl radical, which is readily detected.<sup>29</sup> However, reactions between TBP and the [M<sup>III</sup>H<sub>3</sub>1(O)]<sup>2-</sup> complexes resulted in the protonation of the basic oxo groups to afford the corresponding M<sup>III</sup>–OH complexes (eq 4). Other phenolic substrates (e.g., phenol,



4-methoxyphenol, and 1,4-catechol) reacted in a similar manner. These reactions are consistent with the different pK<sub>a</sub> values for M<sup>III</sup>–OH complexes (Table 1) and phenolic compounds (pK<sub>a</sub> ≈ 18 in DMSO).<sup>14</sup> [Fe<sup>III</sup>H<sub>3</sub>1(OH)]<sup>-</sup> and [Mn<sup>III</sup>H<sub>3</sub>1(OH)]<sup>-</sup> can be deprotonated to afford the M<sup>III</sup>–O complexes when treated with bases, such as KOMe and KOtBu.<sup>30</sup>

## Summary and Conclusions

The analysis of BDE<sub>O-H</sub> for iron and manganese complexes with the same coordination spheres shows that, while both values are less than 80 kcal/mol, the Fe<sup>II</sup>O–H bond is 11 kcal/mol weaker than the Mn<sup>II</sup>O–H bond. This difference in bond strength was corroborated with reactivity studies using various organic substrates, showing the capability of this approach in predicting the reactivity of M–O(H) complexes. A similar trend in O–H bond strength is found for the M(H<sub>2</sub>O)<sub>6</sub> complexes. A BDE<sub>O-H</sub> of 77 kcal/mol has been reported for [Fe<sup>II</sup>(H<sub>2</sub>O)<sub>5</sub>(HO–H)]<sup>2+</sup>,<sup>10b</sup> while we have determined, based on accepted pK<sub>a</sub> and E<sub>1/2</sub> values,<sup>31</sup> that the analogous manganese complex, [Mn<sup>II</sup>–(H<sub>2</sub>O)<sub>5</sub>(HO–H)]<sup>2+</sup>, has a value of 90 kcal/mol (see Supporting Information).

The Fe<sup>III</sup>O–H and Mn<sup>III</sup>O–H complexes have much stronger O–H bonds than their M<sup>II</sup>O–H counterparts, with increases in BDE<sub>O-H</sub> of 33 kcal/mol for [Mn<sup>III</sup>H<sub>3</sub>1(O–H)]<sup>-</sup> and 49 kcal/mol for [Fe<sup>III</sup>H<sub>3</sub>1(O–H)]<sup>-</sup>. These changes in BDE<sub>O-H</sub> are directly related to the increase in the redox potentials of the M<sup>IV/III</sup>–O couples, compared to those for the M<sup>III/II</sup>–OH complexes (Table 1). The BDE<sub>O-H</sub> for the M<sup>III</sup> complexes are statistically the same, with both values above 100 kcal/mol. The strength of the M<sup>III</sup>O–H bonds helps explain the instability of the corresponding M<sup>IV</sup>=O complexes at room temperature, which so far have eluded isolation and prevented us from probing the reactivity of these species.

Current theories for the conversion of water to dioxygen in the OEC of photosynthesis include a terminally coordinated water molecule to a lone manganese center of the tetranuclear cluster.<sup>5</sup> The tyrosyl radical Y<sub>2</sub>O• is proposed to mediate the formation of dioxygen through a series of hydrogen atom transfers. Recent theoretical<sup>23</sup> and X-ray diffraction data<sup>32</sup> cast doubt on this mechanism. For this process to be operative thermodynamically, the homolytic BDE of the MnO–H bonds must be comparable to the ~90 kcal/mol obtained when forming the O–H bond in Y<sub>2</sub>OH. Based only on thermodynamic considerations for an isolated Mn–OH unit, our findings indicate that there is a sufficient driving force for this reaction if Mn<sup>II</sup>–OH and Mn<sup>II</sup>–OH<sub>2</sub> centers are involved. Yet the 110 kcal/mol found for the BDE<sub>O-H</sub> in [Mn<sup>III</sup>H<sub>3</sub>1(OH)]<sup>-</sup> is much higher than that for the O–H bond in a tyrosine, making it thermodynamically unlikely that the direct transfer of a H-atom can happen between an Mn<sup>III</sup>O–H center and a phenolic radical. However, the molecular architecture of our systems differs significantly from the known structural features in the active site of OEC, which could lead to contrasting reactivity. In particular, the unique hydrogen bond cavity that surrounds the M–O(H) unit in [M<sup>III/II</sup>H<sub>3</sub>1(OH)]<sup>-/2-</sup> and [M<sup>III</sup>H<sub>3</sub>1(O)]<sup>2-</sup> should affect their pK<sub>a</sub> and E<sub>1/2</sub> values,<sup>18b-e</sup> which, in turn, may influence the strength of the O–H bonds.<sup>6,21,33</sup> Similar effects may not be present in the active site of OEC. Additional analyses, with both synthetic and protein systems, on the effects of the secondary coordination sphere in metal ions mediated H-atom transfer are necessary before accurate predictions on mechanisms can be made.

- (27) These reactions appear to be enthalpically unfavorable but could proceed if a second, irreversible reaction follows the initial transfer of an H-atom. The BDE<sub>C-H</sub> of 78 kcal/mol for DHA is for the transfer of the first H-atom, while the second H-atom transfer requires only ~43 kcal/mol. This irreversible second step drives the overall reaction towards completion: (a) Mulder, P.; Hemmink, S.; De Heer, M. I.; Lupo, M.; Santoro, D.; Korth, H.-G. *J. Org. Chem.* **2001**, *66*, 6611–6619. (b) Malhotra, R.; McMillen, D. F. *Energy Fuels* **1990**, *4*, 184–193.
- (28) Peduli, G. F.; Lucarini, M.; Pedrielli, P.; Cabiddu, S.; Fattuoni, C. *J. Org. Chem.* **1996**, *61*, 9259–9263.
- (29) Cook, C. D.; Kuhn, D. A.; Fianu, P. *J. Am. Chem. Soc.* **1955**, *78*, 2002–2005.
- (30) pK<sub>a</sub> values of 29.0 and 32 have been reported for MeOH and *t*-BuOH in DMSO.<sup>14</sup>

- (31) (a) Martell, A. E.; Smith, R. M. *Critical Stability Constants*; Plenum: New York, 1976; Vol. IV, p 1. (b) *CRC Handbook of Chemistry and Physics*, 72nd ed.; Lide, D. R., Ed.; CRC Press: Boca Raton, FL, 1991; pp 9–115.
- (32) Zouri, A.; Witt, H. T.; Kern, J.; Fromme, P.; Krauss, N.; Saenger, W.; Orth, P. *Nature* **2001**, *409*, 739–743.
- (33) Blanksby, S. J.; Ellison, G. B. *Acc. Chem. Res.* **2003**, *36*, 255–263.

**Acknowledgment.** Acknowledgment is made to the NIH (GM50781). The authors thank Dr. Thomas Clifford for helpful advice.

**Supporting Information Available:** Descriptions of the  $BDE_{O-H}$  calculations for  $[Mn^{III}H_3I(OH)]^-$ ,  $[Fe^{II}H_3I(OH)]^{2-}$ ,

$[Fe^{III}H_3I(OH)]^-$ , (Schemes S1–S3),  $[Mn^{II}(H_2O)_5(HO-H)]^{2+}$  (Figure S1), and calculated spectra (Figure S2) for the titrations used to determine  $pK(M-OH)$ . This material is available free of charge via the Internet at <http://pubs.acs.org>.

JA030149L